

Deregulation of a Ca^{2+} /calmodulin-dependent kinase leads to spontaneous nodule development

Leïla Tirichine¹, Haruko Imaizumi-Anraku², Satoko Yoshida³, Yasuhiro Murakami², Lene H. Madsen¹, Hiroki Miwa⁴, Tomomi Nakagawa⁵, Niels Sandal¹, Anita S. Albrektsen¹, Masayoshi Kawaguchi⁵, Allan Downie⁴, Shusei Sato⁶, Satoshi Tabata⁶, Hiroshi Kouchi², Martin Parniske³, Shinji Kawasaki² & Jens Stougaard¹

Induced development of a new plant organ in response to rhizobia is the most prominent manifestation of legume root-nodule symbiosis with nitrogen-fixing bacteria. Here we show that the complex root-nodule organogenic programme can be genetically deregulated to trigger *de novo* nodule formation in the absence of rhizobia or exogenous rhizobial signals. In an ethylmethane sulphonate-induced *snf1* (spontaneous nodule formation) mutant of *Lotus japonicus*, a single amino-acid replacement in a Ca^{2+} /calmodulin-dependent protein kinase (CCaMK) is sufficient to turn fully differentiated root cortical cells into meristematic founder cells of root nodule primordia. These spontaneous nodules are genuine nodules with an ontogeny similar to that of rhizobial-induced root nodules, corroborating previous physiological studies¹. Using two receptor-deficient genetic backgrounds we provide evidence for a developmentally integrated spontaneous nodulation process that is independent of lipochitin-oligosaccharide signal perception and oscillations in Ca^{2+} second messenger levels. Our results reveal a key regulatory position of CCaMK upstream of all components required for cell-cycle activation, and a phenotypically divergent series of mutant alleles demonstrates positive and negative regulation of the process.

Spontaneous nodule formation mutants of *Lotus* develop root nodules under rhizobia-free conditions (Fig. 1a). These spontaneous nodules are white and round; they lack the infection threads and bacteroid-containing cells that normally result from rhizobial invasion (Fig. 1b, c). Microscopical analysis show that *snf1-1* nodules, like wild-type rhizobial nodules, have peripheral vascular bundles (Fig. 1d–f), a globular shape, and attachment in root cortex (Fig. 1d, e), and develop from cortical cell divisions abutting vascular xylem poles (Fig. 1g–l). To investigate cellular ontogeny in *snf1-1* further, we took advantage of a *Nin*-GUS promoter fusion to trace the early cell divisions to nodule primordia opposite protoxylem poles (Fig. 1i, l).

When inoculated with *Mesorhizobium loti*, *snf1-1* mutants develop normal bacteria-filled nitrogen-fixing root nodules. In contrast, allelic loss-of-function mutants *ccamk-2* and *ccamk-3* are non-nodulating, whereas *ccamk-1* is leaky. In *ccamk-3* mutants treated with purified Nod-factor, both root hair swelling and root hair deformation were observed (not shown), indicating that Nod-factor perception initiating early cellular and physiological responses occurred. This conclusion was supported by Nod-factor-induced Ca^{2+} oscillations (Supplementary Fig. S1) in *ccamk-2* mutants, showing that a functional CCaMK gene is not required for the induction of Ca^{2+} spiking. A function downstream of Ca^{2+} spiking

was substantiated by an unchanged Nod-factor-dependent Ca^{2+} spiking in *snf1-1* mutant plants (Supplementary Fig. S1).

Legume roots are competent for rhizobial invasion in a zone where root hairs develop and respond maximally to Nod-factor. In inoculated wild-type plants, expression of *Nin*-GUS in root hairs and epidermal cells of this zone requires functional *Nfr1* and *Nfr5* Nod-factor receptors². We used this monitoring system to examine whether *snf1-1* mutants are constitutively activated for early symbiotic responses and to investigate the extent of cellular responses. Inoculation of *snf1-1* mutants carrying a *Nin*-GUS reporter resulted in an expression zone similar to that in *Nin*-GUS wild-type plants. Furthermore, *Nin*-GUS expression was not detected in uninoculated plants or plants inoculated with a Nod-factor-deficient *M. loti nodC* mutant (Fig. 1m–o). This indicates a susceptibility comparable to that of the wild-type and shows that *Nin*-GUS-detectable early signal transduction is dependent on Nod-factor. Later during spontaneous nodule organogenesis, expression was detected in primordial foci and in developing nodule organs in the same way as in rhizobial nodules (Fig. 1p, q). Ectopic expression in root cells was not detected.

Spontaneous nodule development in the absence of exogenous Nod-factor signalling predicts a mutant phenotype that is independent of the *Lotus* NFR1 and NFR5 receptors normally required for electrophysiological responses, Ca^{2+} spiking, root hair deformation and initiation of nodule primordia². To test this hypothesis we analysed the phenotype of *snf1-1 nfr1-1* double mutants: these form spontaneous root nodules in the same way as *snf1-1* mutants (Fig. 2a). *snf1-1* mutants develop up to eight spontaneous nodules, indicating that the conversion of cortical cells into nodule stem cells might be controlled or that subsequent organ development might be regulated. We tested this hypothesis in a hypernodulating *har1-1* genetic background³. In the absence of rhizobia, *snf1-1 har1-1* double mutants developed an average of 15.4 spontaneous nodules, whereas *snf1-1* mutants developed 6.6 nodules and *har1-1* developed none (Fig. 2b). These results indicate that only a few cells dedifferentiate and sustain cell divisions during the *snf1-1* nodule initiation process, which is still autoregulated. In accord with this observation, tissue culture of *snf1-1* explants revealed no gross changes in cell differentiation or phytohormone homeostasis (Supplementary Fig. S2).

Genetic mapping¹ identified the *Lotus* CCaMK gene as a homologue of lily⁴, tobacco⁵ and *Medicago*^{6,7} genes encoding CCaMK. Sequencing of *ccamk-1*, *ccamk-2*, *ccamk-3*, *ccamk-4* (refs 8–10) and *snf1-1* mutant alleles identified an allelic series. Single-nucleotide mutations led to a stop codon in *ccamk-2*, generating a truncated protein carrying one EF-hand, and to the substitution of Gly30 (G30E) in *ccamk-3* and Ser25 (S25F) in *ccamk-4* (Supplementary

¹Laboratory of Gene Expression, Department of Molecular Biology, University of Aarhus, Gustav Wieds Vej 10, DK-8000 Aarhus C, Denmark. ²National Institute of Agrobiological Sciences, Kannondai, Tsukuba, Ibaraki 305-8602, Japan. ³University of Munich, Department of Biology I, Genetics, Maria-Ward-Strasse 1a, D-80638 München, Germany. ⁴John Innes Centre, Colney, Norwich NR4 7UH, UK. ⁵University of Tokyo, Department of Biological Sciences, Graduate School of Science, Hongo, Bunkyo-ku, Tokyo 113-0033, Japan. ⁶Kazusa DNA Research Institute, Kisarazu, Chiba, 292-0818, Japan.

Table S1). A 299-base-pair duplication was found in *ccamk-1*. In *snf1-1*, C → T transitions led to the replacement of Thr 265 by isoleucine and a mutation in intron 1 (Fig. 3a, and Supplementary Table S1). The *Lotus* CCaMK gene comprises seven exons (Fig. 3a), and Southern hybridization indicates a single-copy gene.

To access each *snf1-1* mutation individually, transformation constructs carrying only the T265I substitution (*snf1-2*) or the intron mutation (*snf1-3*) were made by site-directed mutagenesis. Spontaneous nodulation was observed on *Agrobacterium rhizogenes* transgenic roots of *ccamk-2* mutants transformed with constructs carrying either *snf1-2* or both point mutations (*snf1-1*). Neither the intron 1

mutation (*snf1-3*) nor the wild-type gene conferred spontaneous nodulation (Supplementary Table S2b). All four constructs complemented *ccamk-2* for rhizobial nodulation, showing that they encode a CCaMK protein performing its positive function (Supplementary Table S2a, Fig. 2c). Spontaneous nodulation obtained with *snf1-2* constructs confirms that spontaneous organogenesis is caused by mutational change of CCaMK protein properties. Further support for this conclusion comes from the dominant-negative effect observed in *snf1-1* mutants transformed with the wild type or the *snf1-3* mutant (Supplementary Table S2c).

Expression of CCaMK is organ regulated. In comparison with leaves, stems and cotyledons, a 25-fold higher transcript level was found in uninoculated roots and in nodules (Fig. 3b). Expression is affected only marginally by inoculation with *M. loti* (Fig. 3c). To investigate whether the transcription of CCaMK was limiting nodulation, we determined transcript levels in hypernodulating *har1-5* *Lotus* mutants, in which nodule initiation and organogenesis are unrestricted by autoregulation. Only minor variations in expression between uninoculated and inoculated wild type on the one hand and *har1-5* on the other (Fig. 3d) indicate that transcription of CCaMK might not be upregulated in hypernodulating mutants and is unlikely to be a limiting factor in wild-type plants. Autoregulation of spontaneous nodulation revealed in *snf1-1 har1-1* double mutants (Fig. 2b) seems not to be a simple transcriptional regulation of CCaMK.

The conceptual CCaMK protein consists of 518 amino-acid residues (Fig. 4a, b, and Supplementary Fig. S3). A possible nuclear localization sequence is followed by a serine/threonine kinase domain¹¹, a calmodulin (CaM)-binding/autoinhibition domain and three, or possibly four, visinin-like EF-hands (Fig. 4a, b). The point mutation in *snf1-1* leads to the replacement of Thr 265 by isoleucine. In lily CCaMK, the corresponding Thr 267 is the only site

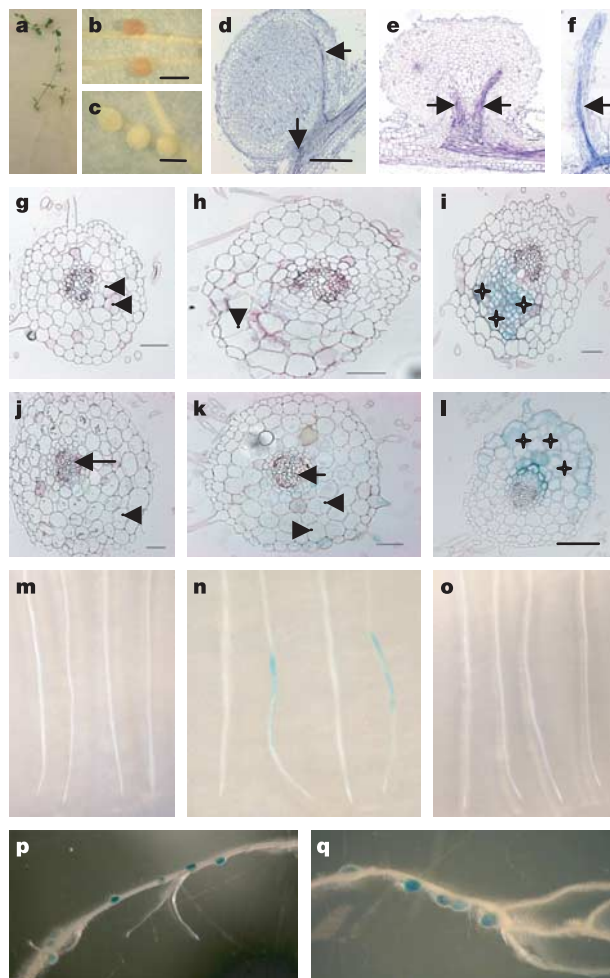


Figure 1 | Phenotype of *snf1-1* mutants and ontogeny of spontaneous nodules. **a**, *Lotus* wild-type and *snf1-1* (right). **b**, *M. loti* wild-type nodules. **c**, Spontaneous *snf1-1* nodules. **d**, Section of wild-type nodule. **e**, Spontaneous nodule. **f**, Lateral root. Black arrows indicate peripheral vascular bundles in nodules and central root vasculature. **g–i**, Transverse sections of wild-type *M. loti* nodule primordia. **g**, Initial cell division in the outer cortex; **h**, cell divisions in pericycle and cortex; **i**, later stage nodule primordium formed by the cell divisions in pericycle and cortex. In **g** and **h**, arrowheads indicate cells dividing opposite the xylem pole. **j–l**, Sections of spontaneous nodule primordia. **j**, Initial cell division in outer cortex; **k**, cells dividing in cortex and the pericycle; **l**, spontaneous nodule primordium formed by cells dividing in pericycle and cortex. In **j** and **k**, arrows indicate xylem poles; in **j** and **k**, arrowheads indicate pericycle and cortex cells dividing opposite xylem poles. **i**, **l**, Primordia cells are blue (stars) as a result of *Nin*-GUS activity. **m–o**, GUS activity in (from left to right) wild-type, wild-type *Nin*-GUS, *snf1-1* and *snf1-1 Nin*-GUS roots. **m**, Uninoculated. **n**, *M. loti*. **o**, *M. loti* *NodC*. **p**, **q**, *Nin*-GUS activity in wild-type rhizobial nodules (**p**) and spontaneous nodules (**q**). Scale bars, 1 mm (**b**, **c**); 100 μ m (**d**, **j**); 50 μ m (**h**, **k**, **l**); 20 μ m (**g**, **i**).

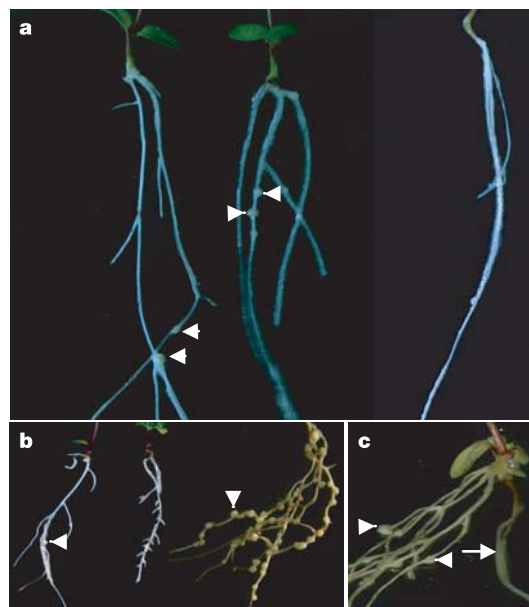


Figure 2 | Nod-factor receptor-independent development of spontaneous nodules and complementation of the *ccamk-2* loss of function mutation. **a**, From left to right: spontaneous nodules on *snf1-1* mutants, spontaneous nodules on *nfr1-1 snf1-1* double mutants, and *nfr1-1* control roots without nodules. **b**, From left to right: spontaneous nodules on *snf1-1* mutants, *har1-1* control roots without nodules, and spontaneous nodules on *snf1-1 har1-1* double mutants. Arrowheads indicate spontaneous nodules five weeks after germination. **c**, Spontaneous nodules on transgenic *ccamk-2* roots transformed with *snf1-1*. Arrowheads show hairy roots with spontaneous nodules. The arrow indicates the non-transgenic main root without spontaneous nodules.

for Ca²⁺-dependent autophosphorylation¹²⁻¹⁴. Studies *in vitro* show that lily CCaMK is activated by the binding of Ca²⁺ at EF-hands, causing increased affinity for CaM and release of autoinhibition, yielding a CCaMK with maximum substrate phosphorylation activity. This biochemical mechanism indicates that the primary activation of CCaMKs might occur in response to Ca²⁺ fluxes¹³⁻¹⁵.

To determine the responsiveness of *Lotus* CCaMK to Ca²⁺ and CaM, wild-type CCaMK, G30E (*ccamk-3*) or T265I (*snf1-2*)-tagged proteins were purified from *Escherichia coli* and assayed *in vitro*. Wild-type CCaMK protein shows a twofold Ca²⁺-stimulated increase in autophosphorylation, and substrate phosphorylation is accelerated by the addition of CaM (Fig. 4c, d). The level of *in vitro* autophosphorylation increased exponentially rather than linearly with increasing CCaMK concentration, indicating an intermolecular mechanism for autophosphorylation (Fig. 4e, and Supplementary Fig. S4). Autophosphorylation activities of G30E and T265I mutant proteins were undetectable (Fig. 4c). In a likely model, the positive regulatory role of CCaMK is triggered by Nod-factor-induced Ca²⁺ fluxes. This positive function is lost in *ccamk-2*, *ccamk-3* and *ccamk-4* mutants. However, the CCaMK T265I protein retains this positive regulatory role, indicating that a level of substrate phosphorylation activity lower than that in the wild-type (Fig. 4c), stimulated by Ca²⁺ and CaM, might be sufficient for nodulation.

Lack of autophosphorylation in the T265I mutant protein implies that autophosphorylation of CCaMK is dispensable for nodulation. The corresponding observation has been made for rhizobial nodulation of *Medicago truncatula*¹⁶. The fact that *snf1-1* is a recessive allele and the negative effect of the wild-type gene in *snf1-1* mutants (Supplementary Table S2c), indicate that wild-type CCaMK suppresses spontaneous *snf1-1* nodulation. CCaMK therefore seems to be under negative regulation. In *snf1-1* mutants negative regulation could be lost by conformational changes reminiscent of the signalling without kinase activity reported for an amino-acid-substituted tomato Pto (*Pseudomonas syringae* pv. *tomato* resistance) kinase¹⁷.

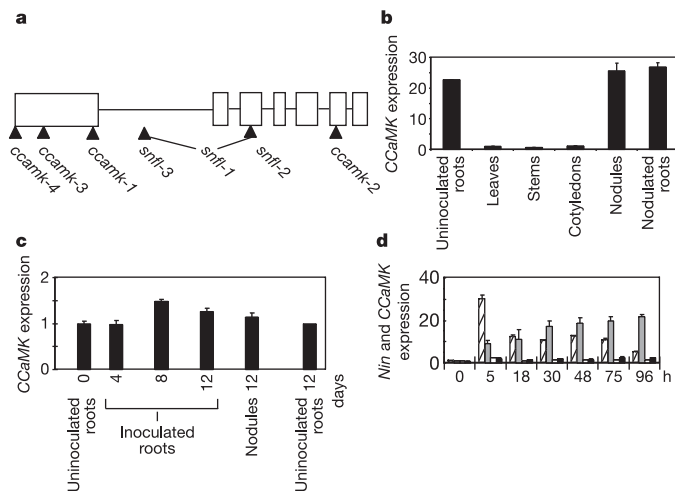


Figure 3 | The CCaMK gene and expression of CCaMK and *Nin* in wild-type and hypernodulation *har1-5* mutants. **a**, CCaMK gene structure. Open boxes, exons; lines, introns; black triangles, mutations in *snf1-1* and *ccamk-4* alleles. **b**, Steady-state CCaMK transcript level in root, leaf, stem, cotyledon, nodule and root segments from nodulated root. **c**, CCaMK transcripts in roots, roots after 12 days, roots 4–12 days after inoculation with *M. loti* and nodules at 12 days. **d**, CCaMK and *Nin* transcripts in wild-type and *har1-5* uninoculated roots, and roots inoculated for 5–96 h. Hatched columns, *Nin* expression in wild type; grey columns, *Nin* expression in *har1-5*; open columns, CCaMK expression in wild type; black columns, CCaMK expression in *har1-5*. Results are fold increase compared with leaves (**b**) and uninoculated roots (**c**, **d**). Error bars represent standard deviations from three independent experiments.

Alternatively, the autophosphorylation-induced inactivation associated with lily CCaMK¹⁵ protein aggregation could act negatively. It is unclear whether this aggregation occurs *in vivo*, but according to this mechanism the activity of CCaMK might be determined by the balance between activation by phosphorylation and aggregation. Lack of autophosphorylation in *snf1-1* and *snf1-2* leaves CCaMK in a ground state where activity is minimal but sufficient to trigger downstream signal transduction arising from a lack of autophosphorylation-dependent aggregation. According to this model, basal autophosphorylation in the wild type is sufficient for aggregation and CCaMK inactivation. Absence of autophosphorylation and aggregation in lily CCaMK, where Thr 267 is replaced by alanine, supports this hypothesis¹⁵. Spontaneous nodulation of *M. truncatula* with decreased CCaMK activity supports the notion that a CCaMK activity that is less than maximal triggers downstream events¹⁶.

Intermolecular autophosphorylation is indicated by our *in vitro*

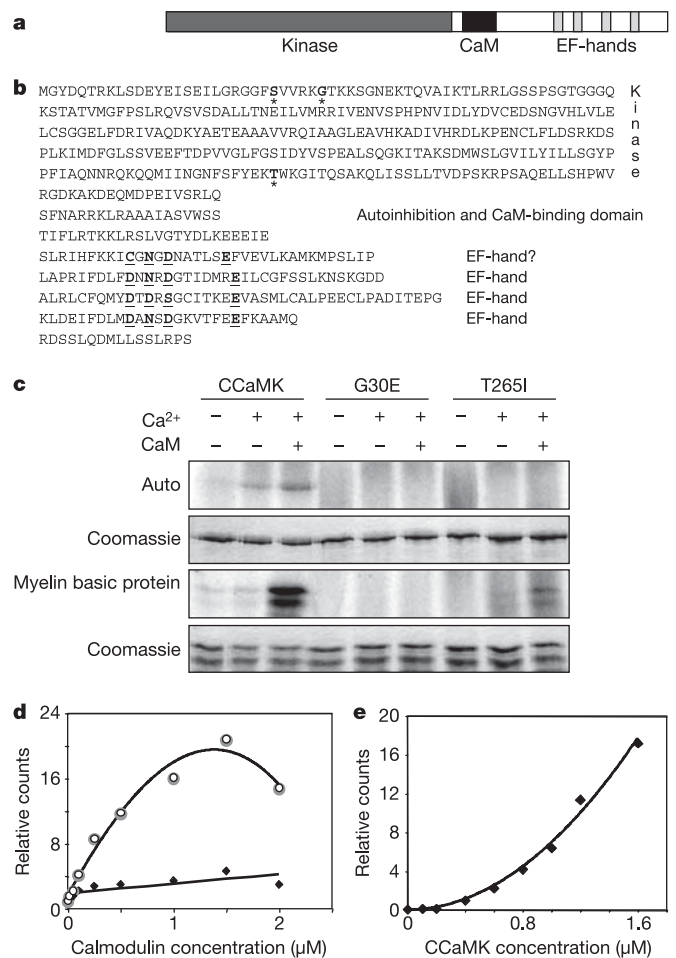


Figure 4 | Domains and *in vitro* kinase activity of CCaMK protein. **a**, CCaMK domains. **b**, Amino acids arranged in protein domains. Bold residues with asterisk, autophosphorylation sites and amino acids substituted in mutants; bold underlined residues, conserved EF-domain residues. **c**, Autophosphorylation (auto) and substrate phosphorylation (myelin basic protein) of CCaMK, G30E and T265I proteins in the presence and absence of Ca²⁺ and CaM. Corresponding Coomassie staining is also shown as indicated. **d**, Effects of CaM on CCaMK autophosphorylation and substrate phosphorylation. Radioactivity incorporated into CCaMK protein was quantified and is presented relative to signal without CaM. Diamonds, autophosphorylation; circles, phosphorylation of myelin basic protein. **e**, Protein concentration-dependent autophosphorylation. Radioactivity incorporated into CCaMK is presented relative to a sample containing 0.4 μM CCaMK.

assays, and data from lily imply that active CCaMK is a multimeric enzyme¹⁴. This is consistent with the recessive nature of *snf1-1* and the dominant-negative effect of wild-type CCaMK in transgenic *snf1-1* (Supplementary Table S2c). Heterozygotes and hemizygotes would still make multimeric protein with sufficient wild-type subunits to behave in the same way as wild-type CCaMK. Supporting this notion is the observation that *snf1-1* shows penetrance in about 2.5% of heterozygous *wt/snf1-1* plants that develop spontaneous nodules, conceivably after the assembly of multimeric complexes with sufficient T265I subunits to escape negative regulation.

We show that CCaMK is necessary and sufficient for dedifferentiation of root cortical cells into nodule initials. Spontaneous nodulation of *nfr1-1 snf1-1* double mutants is direct evidence for Nod-factor-independent organ development resulting from a single amino-acid substitution. This provides compelling evidence for a pivotal role of mechanisms regulating CCaMK activity, and we infer that any parallel signal transduction pathways downstream of Nod-factor perception, or other signals from rhizobia required for the initiation of nodule primordia, seem to converge at or above CCaMK activation. Our results support a direct signal transduction mechanism from Nod-factor perception to meristem formation. This identification of the genetic switch for nodule organogenesis has significant biotechnological potential.

METHODS

Plant material. All mutants described are in the ecotype Gifu B-129 background. The *snf1-1* allele was isolated¹ after mutagenesis with ethylmethane sulphonate¹⁸, and *ccamk-1*, *ccamk-2*, *ccamk-3* and *ccamk-4* were previously called *sym15-1*, *sym15-2* (ref. 8), *sym72-1* and *sym72-2* (ref. 9). Plants were grown with or without *M. loti*, strain NZP2235 or MAFF30-3099.

Microscopic analysis. Nodules and root tissues were prepared for microscopic analysis as described previously¹.

Complementation. For *in planta* complementation, a genomic fragment containing the CCaMK gene including a 3.1-kilobase promoter region and a 3' region of 1.3 kilobases was inserted into the pIV10 plasmid. Triparental transfer of construct into *A. rhizogenes* strain AR12, and AR1193 and 'hairy root' transformation were performed as described previously².

Other methods. The double-mutant analysis, *Nim*-GUS reporter lines, expression analysis and *in vitro* kinase assays are described in Supplementary Methods S5.

Received 16 March; accepted 5 May 2006.

1. Tirichine, L., James, E. K., Sandal, N. & Stougaard, J. Spontaneous root nodule formation in the model legume *Lotus japonicus*: A novel class of mutants nodulates in absence of *Rhizobium*. *Mol. Plant Microbe Interact.* **19**, 373–382 (2006).
2. Radutoiu, S. *et al.* Plant recognition of symbiotic bacteria requires two LysM receptor-like kinases. *Nature* **425**, 585–592 (2003).
3. Krusell, L. *et al.* Shoot control of root development and nodulation is mediated by a receptor-like kinase. *Nature* **420**, 422–426 (2002).
4. Patil, S., Takezawa, D. & Poovaiah, B. W. Chimeric plant calcium/calmodulin-dependent protein kinase gene with a neural visinin-like calcium-binding domain. *Proc. Natl Acad. Sci. USA* **92**, 4897–4901 (1995).
5. Liu, Z., Xia, M. & Poovaiah, B. W. Chimeric calcium/calmodulin-dependent protein kinase in tobacco: differential regulation by calmodulin isoforms. *Plant Mol. Biol.* **38**, 889–897 (1998).
6. Levy, J. *et al.* A putative Ca²⁺ and calmodulin-dependent protein kinase required for bacterial and fungal symbioses. *Science* **303**, 1361–1364 (2004).
7. Mitra, R. M. *et al.* A Ca²⁺/calmodulin-dependent protein kinase required for symbiotic nodule development: Gene identification by transcript-based cloning. *Proc. Natl Acad. Sci. USA* **101**, 4701–4705 (2004).
8. Schausser, L. *et al.* Symbiotic mutants deficient in nodule establishment identified after T-DNA transformation of *Lotus japonicus*. *Mol. Gen. Genet.* **259**, 414–423 (1998).
9. Senoo, K. *et al.* Isolation of two different phenotypes of mycorrhizal mutants in the model legume plant *Lotus japonicus* after EMS-treatment. *Plant Cell Physiol.* **41**, 726–732 (2000).
10. Kawaguchi, M. *et al.* Root, root hair, and symbiotic mutants of the model legume *Lotus japonicus*. *Mol. Plant Microbe Interact.* **15**, 17–26 (2002).
11. Schenk, P. W. & Snaar-Jagalska, B. E. Signal perception and transduction: The role of protein kinases. *Biochim. Biophys. Acta* **1449**, 1–24 (1999).
12. Takezawa, D., Ramachandiran, S., Paranjape, V. & Poovaiah, B. W. Dual regulation of a chimeric plant serine/threonine kinase by calcium and calcium/calmodulin. *J. Biol. Chem.* **271**, 8126–8132 (1996).
13. Sathyanarayanan, P. V., Cremona, C. R. & Poovaiah, B. W. Plant chimeric Ca²⁺/calmodulin-dependent protein kinase. Role of the neural visinin-like domain in regulating autophosphorylation and calmodulin affinity. *J. Biol. Chem.* **275**, 30417–30422 (2000).
14. Sathyanarayanan, P. V., Siems, W. F., Jones, J. P. & Poovaiah, B. W. Calcium-stimulated autophosphorylation site of plant chimeric calcium/calmodulin-dependent protein kinase. *J. Biol. Chem.* **276**, 32940–32947 (2001).
15. Sathyanarayanan, P. V. & Poovaiah, B. W. Autophosphorylation-dependent inactivation of plant chimeric calcium/calmodulin-dependent protein kinase. *Eur. J. Biochem.* **269**, 2457–2463 (2002).
16. Gleason, C. *et al.* Nodulation independent of rhizobia induced by a calcium-activated kinase lacking autoinhibition. *Nature* doi:10.1038/nature04812 (this issue).
17. Rathjen, J. P., Chang, J. H., Staskawicz, B. J. & Michelmore, R. W. Constitutively active *Pto* induces a *Prf*-dependent hypersensitive response in the absence of *avrPto*. *EMBO J.* **18**, 3232–3240 (1999).
18. Perry, J. A. *et al.* TILLING reverse genetics tool and a web-accessible collection of mutants of the legume *Lotus japonicus*. *Plant Physiol.* **131**, 866–871 (2003).

Supplementary Information is linked to the online version of the paper at www.nature.com/nature.

Acknowledgements We thank Finn Pedersen for plant care and crossing.

Author Information The sequences for the *L. japonicus* ecotype GIFU CCaMK gene and mRNA are deposited in the EMBL nucleotide database under accession numbers AM230792 and AM230793. Reprints and permissions information is available at npg.nature.com/reprintsandpermissions. The authors declare no competing financial interests. Correspondence and requests for materials should be addressed to J.S. (stougaard@mb.au.dk).